






Design of Integrating Sphere Uniform Light System for Solar Simulator

Jiali Chen, Gaofei Sun , Shi Liu , Guoyu Zhang, Siwen Chen , Jierui Zhang , and Qiang Liu 

Abstract—In the process of designing and adjusting the solar simulator, the side lobe effect and aberration of the optical integrator affect the irradiation uniformity, an integrating sphere is proposed to replace the optical integrator for uniform light and the compound parabolic reflector for beam shaping. First, based on the equal illuminance theorem and the radiation transfer theory, the calculation formula of the energy transmission efficiency of the porous integrating sphere is derived; Then, the light hole illuminance interference factor is introduced, and the effects of the aperture size of the integrating sphere, the radius of the integrating sphere, and the size and position of the baffle on the energy transmission efficiency and irradiation uniformity are analyzed. Finally, an integrating sphere uniform light system with high energy transmission efficiency and uniformity is designed and simulated with LightTools software. The simulation results show that: the average difference of irradiation uniformity and the range difference of irradiation uniformity are closest to 1 in the area where the ratio of the opening size and radius of the integrating sphere is 36%–40%, and the light is evenly distributed; When the baffle position is 0.8 times of integrating sphere radius away from the light entrance hole, irradiation non-uniformity at the outlet hole is 1.99%, which is the best position of the baffle; In the effective irradiation surface of $\Phi 1032$ mm, the irradiation non-uniformity is 1.98%, and the maximum irradiance is 0.62 solar constants, the spot simulation with high irradiation uniformity on large irradiation surface is realized.

Index Terms—Solar simulation, integrating sphere, energy transmission efficiency, irradiation non-uniformity, large irradiation surface.

I. INTRODUCTION

FROM aerospace to thermal vacuum and thermal balance test of spacecraft, on orbit illumination test of space optical

Manuscript received 23 September 2022; revised 5 January 2023; accepted 16 January 2023. Date of publication 18 January 2023; date of current version 1 February 2023. This work was supported by the Jilin Provincial Science and Technology Development Plan under Grant 20210201034GX. (Corresponding author: Gaofei Sun.)

Jiali Chen, Siwen Chen, Jierui Zhang, and Qiang Liu are with the Key Laboratory of Opto-electronic Measurement and Optical Information Transmission Technology, Ministry of Education, Department of Instrumentation Science and Technology, Changchun University of Science and Technology, Changchun 130022, China (e-mail: 935825623@qq.com; 52107218@qq.com; jierui_zhang_zjr@163.com; 874982570@qq.com).

Gaofei Sun, Shi Liu, and Guoyu Zhang are with the Key Laboratory of Opto-electronic Measurement and Optical Information Transmission Technology, Ministry of Education, Department of Instrumentation Science and Technology, Changchun University of Science and Technology, Changchun 130022, China, also with the Institute of Aerospace Ground Simulation Test and Testing Technology, Changchun University of Science and Technology, Changchun 130022, China, and also with the Optical Measurement and Control Instrumentation, Jilin Province Engineering Research Center, Changchun 130022, China (e-mail: 821323880@qq.com; 1136795466@qq.com; zh_guoyu@163.com).

Digital Object Identifier 10.1109/JPHOT.2023.3237931

remote sensor; To new energy photovoltaic, improve the accuracy of detection and calibration of solar arrays, and build space solar power stations; From agricultural science to frozen soil and ice research and the construction of artificial solar houses for irradiating plants, it is necessary to use solar simulators to carry out ground simulation tests. Among them, the irradiation uniformity of the solar simulator is an important basis for determining whether the design of the solar simulator is reasonable [1], and is also the key data in the application field.

At present, symmetrical optical integrators are widely used in the uniform light system of the solar simulator. In order to realize the simulation of uniform light spots on large irradiation surfaces, researchers have analyzed and optimized the integrators' aberrations and designed subsequent projection systems, for example, the large area projection solar simulator developed by Du Zhiqiang [2] and others has an irradiation non-uniformity of $\pm 4.26\%$ in the 1000 mm \times 1000 mm effective irradiation surface, however, the projection system is a large aberration system, and the process of correcting the field curvature and distortion generated by it is complex and demanding. In order to further improve uniformity and solve the problems of superimposed image position error, poor optical axis consistency between element lenses corresponding to field lens group and projection lens group and stray light interference caused by human error and other factors during optical integrator processing and assembly [3], [4], some researchers have also improved the structure of the optical integrator. For example, the beam type optical integrator developed by Li Zhiqiang [5] and others, the light of each channel of the integrator field mirror and the projection mirror group is one-to-one corresponding and opaque to each other, which solves the disadvantage that it is difficult to ensure the consistency of the optical axis during installation and adjustment, however, the irradiation uniformity at the edge of the spot is poor. The outlet pupil optical integrator developed by Katsuki [6] and others solves the imaging blur caused by the position error of the superimposed image, but cannot compensate for the edge light. In addition, the optical integrator is always limited by the material and structure, constraint of beam incidence angle and the irradiation uniformity and irradiance are mutually restricted. There are problems such as its inability to correct aberration, side lobe effect and the irradiance and irradiance uniformity under the large irradiation surface cannot be further improved [7], which affect the development of the large irradiation surface solar simulator.

Therefore, the aim of this paper is to improve the irradiation uniformity of large irradiation surface, based on the equal

illuminance theorem and the radiation transfer theory, the light hole illuminance interference factor is introduced, an integrating sphere is proposed to replace the optical integrator as a uniform light system, the calculation model of energy transmission efficiency of integrating sphere with multiple openings is established, the influence of aperture size and radius ratio of integrating sphere on irradiation surface uniformity is analyzed, design a reasonable integrating sphere uniform light system, it solves the problem that the uniformity of optical integrator is greatly affected by the angle of incident light, the integration sphere uniform effect with high energy transmission efficiency and high uniformity is realized.

II. ANALYSIS OF THE INFLUENCE OF SPHERICAL ABERRATION, SIDE LOBE, IRRADIATION SURFACE AND IRRADIANCE ON IRRADIATION UNIFORMITY

The optical integrator of traditional solar simulator is mainly composed of field mirror, projection mirror and focusing lens [4]. Ideally, the optical integrator is placed at the second focal point of the ellipsoidal condenser and receives the light converged by the ellipsoidal condenser and incident at a certain angle [8], after it is divided by the field mirror lens and superimposed by the projection mirror lens, the light beam exits in the form of uniform distribution to achieve uniform treatment of the irradiation spot. In practice, in order to achieve good light uniformity, the angle, spatial distribution and beam intensity of incident light are required to be high, but it is difficult to meet the requirements. Due to the limitation of materials and structures, the optical integrator itself cannot correct aberrations. Sometimes, in order to shorten the axial optical system size, the relative aperture of the integrator needs to be increased, which increases the influence of aberrations on the optical integrator's uniform effect [9]; Since the focusing lens is shared by all optical channels, the relative positions of the focusing lens and the projection mirror lens in each optical channel are not strictly consistent, and the imaging of the integrator loses strict axisymmetry [9]; Because of the large spherical aberration of the integrator diaphragm, the incident light with large angle will be disorderly strung into harmful stray light in the adjacent sub lenses of the optical integrator projection mirror, resulting in side lobe effect [10], [11], [12], [13]; Because the number of sub lenses of the optical integrator limits the light uniform effect of the integrator, the more the number of sub lenses, the larger the irradiation surface will be and the subdivided beam will be emitted more uniformly, but at the same time, the irradiance will be reduced, that is, the irradiation surface, the irradiation uniformity and the irradiance are mutually restricted [9]. Moreover, the above problems are caused by the working principle of the optical integrator, resulting in the reduction of irradiation uniformity and irradiance loss at the effective irradiation surface, which is difficult to be fully optimized by design.

Therefore, the principle of integrating sphere uniform light principle is studied in this paper; A method of using the compound parabolic concentrator inversely as the compound parabolic reflector [14] for beam shaping is proposed; An

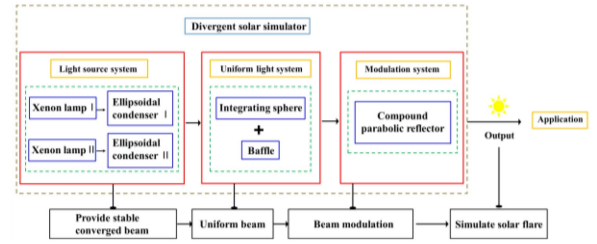


Fig. 1. Optical system of composition diagram.

TABLE I
MAIN TECHNICAL INDICES

Item	Target
Illumination area	$\leq \Phi 1000\text{mm}$
Non-uniformity	$\leq 3\%$
Irradiance	$\leq 0.5S_0$
Energy transmission efficiency of integrating sphere	$\leq 45\%$

integrating sphere uniform light system is designed to replace the optical integrator; Solve the problems of irradiation surface, irradiation uniformity and irradiance mutual restriction and side lobe effect of optical integrator; The solar irradiation simulation with high irradiation uniformity under large irradiation surface is realized.

III. COMPOSITION AND WORKING PRINCIPLE OF OPTICAL SYSTEM OF SOLAR SIMULATOR BASED ON INTEGRATING SPHERE

The optical system of the solar simulator based on the integrating sphere is mainly composed of xenon lamp array, ellipsoidal condenser array, integrating sphere, baffle and compound parabolic reflector, the composition of the optical system is shown in Fig. 1.

Among them, the angle, spatial distribution and beam intensity of the incident light of the integrating sphere will not affect the uniform light effect of the integrating sphere [15], place it at the second focal point of the ellipsoidal condenser, and the light beam converged by the ellipsoidal condenser enters the integrating sphere and forms a uniform spot at the light outlet hole after several diffuse reflections. The light inlet of the compound parabolic reflector is connected with the light outlet of the integrating sphere, its high symmetry and beam are reflected on the inner wall, the corresponding action of the annulus makes the irradiation on the irradiation surface evenly distributed. Finally, the spot simulation with large irradiation surface and high irradiation uniformity is realized. This structure can also solve the problem that the small aperture integrating sphere emits a large irradiation surface. The main technical indicators are shown in Table I.

IV. DESIGN OF INTEGRATING SPHERE WITH HIGH ENERGY TRANSMISSION EFFICIENCY AND UNIFORMITY

A. Analysis and Design of the Influence of the Entrance and Outlet Holes of the Integrating Sphere on the Energy Transmission Efficiency

According to the diffuse reflection theory and the equal illumination theorem [16], when the incident radiation flux is $\phi_{s-input}$, the light is diffused in the integrating sphere for several times, the output radiation flux $\phi_{s-output} = EA_{Hp}$, the formula is shown in (1).

$$\phi_{s-output} = \frac{\phi_{s-input}\rho}{A_s[1 - \rho(1 - f_{all})]} \cdot \pi R^2 [1 - (1 - 2f_{eff})^2] \quad (1)$$

Where, R is the radius of the integrating sphere; ρ is the reflectivity of the coating on the inner wall of the integrating sphere; A_s is the inner surface area of the integrating sphere; A_{Hp} is the plane area of the opening, derivation from the formula of space solid angle and plane geometry; f_{eff} is the effective opening ratio of the integrating sphere representing the open hole ratio that only calculates the size of the optical hole, $f_{eff} = \frac{\sum_{j=0}^n (R - \sqrt{R^2 - r_j^2})}{2R}$; f_{all} is the total opening ratio representing the open hole ratio that includes the size of the incoming optical hole and the size of the outgoing optical hole, $f_{all} = \frac{\sum_{i=0}^n (R - \sqrt{R^2 - r_i^2}) + \sum_{j=0}^n (R - \sqrt{R^2 - r_j^2})}{2R}$; i is the number of light entrance holes; j is the number of light outlet holes; r_i is the radius of the light entrance hole of the integrating sphere; r_j is the radius of the light outlet hole of the integrating sphere.

The energy transmission efficiency of the integrating sphere is defined as $\eta_{sp} = \frac{\phi_{s-output}}{\phi_{s-input}}$, then the η_{sp} expression is

$$\eta_{sp} = \frac{\rho \left(\frac{r_j}{R}\right)^2}{4 - 2\rho \left[\sqrt{1 - \left(\frac{r_i}{R}\right)^2} + \sqrt{1 - \left(\frac{r_j}{R}\right)^2} \right]} \quad (2)$$

Where, ρ is the reflectivity of the coating on the inner wall of the integrating sphere, Poly tetra fluoroethylene is selected as the inner coating material of integrating sphere [17], $\rho = 0.98$; R is the radius of the integrating sphere.

From the above formula, the energy transmission efficiency is affected by the size of the light entrance hole, the size of the light entrance hole and its own radius of the integrating sphere. This formula can also serve as a reference for the subsequent design of the opening size and other parameters of the integrating sphere. Next, the specific opening size and radius of the integrating sphere are reasonably analyzed and designed.

First, the size of the light entrance hole determines the energy of the light source that enters the integrating sphere after being converged by the ellipsoidal condenser and the energy of the light that directly escapes after entering the integrating sphere after being reflected by the baffle. Therefore, in the design, the light beam emitted from the front light source system should be received as much as possible and the reduction of the energy transmission efficiency of the integrating sphere caused by the large aperture should be avoided. Since the xenon lamp ellipsoidal condenser light source system irradiates the surface at the

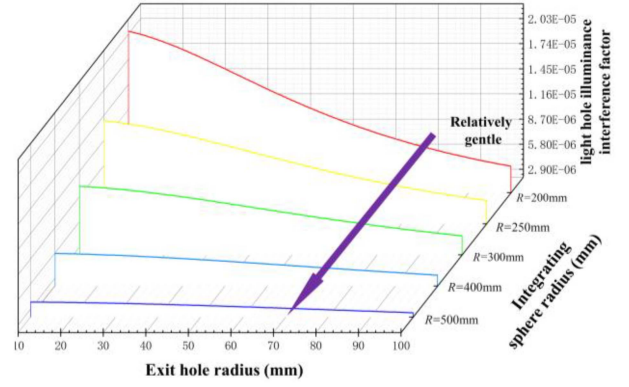


Fig. 2. Diagram of the relationship between the size of the light outlet hole of the integrating sphere and the illumination interference factor of the light outlet hole.

bifocal plane $\Phi < 40$ mm, so in order to ensure that all light can enter the integrating sphere and avoid the escape of light caused by the large light entrance hole of the integrating sphere, the diameter of the light entrance hole of the integrating sphere is $\Phi \geq 40$ mm, so the radius of the light entrance hole of the integrating sphere is 20 mm.

Second, the position of the light outlet hole has no significant effect on its optical characteristics, which can be determined by the use structure of the integrating sphere [18]. Therefore, the structure should be simplified as much as possible, and the light outlet hole and the light entrance hole of the integrating sphere should keep the optical axis consistent. However, its size affects the energy transmission efficiency and uniform effect of the integrating sphere.

From the expression of total opening ratio, the ratio of the actual diffuse reflection layer area of the integrating sphere to the ideal diffuse reflection layer area is shown in (3), the light hole illuminance interference factor of the integrating sphere is defined as $K_R = \frac{E}{E_0} \rho(1 - f)$ [19], it shows that the irradiance at the light outlet hole is affected by the aperture ratio of the integrating sphere, the reflectivity of the inner wall and the illuminance of the light source. The larger the value, the more the illuminance at the light hole is attenuated, and the smaller the value, the less the interference, the formula is shown in (4).

$$f = 1 - \frac{\sqrt{R^2 - r_i^2} + \sqrt{R^2 - r_j^2}}{2R} \quad (3)$$

$$K_R = \frac{\phi_{s-input}\rho^2 \left[\sqrt{1 - \left(\frac{r_i}{R}\right)^2} + \sqrt{1 - \left(\frac{r_j}{R}\right)^2} \right]}{16\pi R^2 E_0 \left[2 - \rho \left(\sqrt{1 - \left(\frac{r_i}{R}\right)^2} + \sqrt{1 - \left(\frac{r_j}{R}\right)^2} \right) \right]} \quad (4)$$

Where, E_0 is the illuminance of xenon lamp light source.

Take integrating sphere radius of 200 mm, 250 mm, 300 mm, 400 mm and 500 mm respectively, analyze the influence of different sizes of light outlet holes on the irradiance of light outlet holes in (4), and make the relationship diagram as shown in Fig. 2.

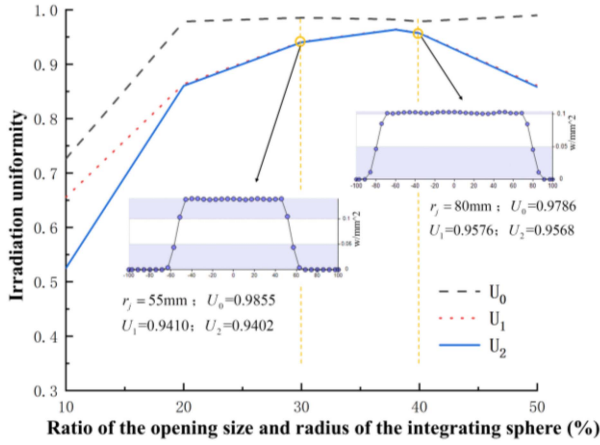


Fig. 3. The influence of the size of the light hole of the integrating sphere on the irradiation uniformity.

It can be seen from Fig. 2 that the existence of the light outlet hole reduces the diffuse reflection area of the light inside the integrating sphere, and does not achieve a perfect uniform light effect; Arrows indicate that as the radius increases, the attenuation of illumination at the outlet hole is compensated to some extent. The radius of the best integrating sphere light outlet hole is in the range of 70 mm–100 mm, and the illuminance interference factor is small and relatively gentle in this range.

B. Analysis and Design of the Influence of the Entrance and Outlet Holes of the Integrating Sphere on the Uniform Effect

At this time, the light entrance hole of the integrating sphere is only used as the opening for receiving the light source, so it is relatively small relative to the size of the light outlet hole and the radius of the integrating sphere, which has little effect on the uniform light effect of the integrating sphere and can be ignored [19]. In order to discuss the influence of the size of the integrating sphere's light outlet hole on the irradiation uniformity, a model was established using LightTools to simulate and analyze the irradiation uniformity at the integrating sphere's light outlet hole under different aperture and radius ratios. Generally, the irradiation uniformity is judged by the average difference of irradiation uniformity U_0 , the range difference of irradiation uniformity U_1 , the range difference of irradiation uniformity U_2 and the irradiation non-uniformity *Bias* [19], [20], [21].

$$\begin{cases} U_0 = \frac{E_{av}}{E_{max}} \\ U_1 = \frac{E_{max} - E_{min}}{E_{max}} \\ U_2 = 1 - \frac{E_{max} - E_{min}}{E_{av}} \\ Bias = \pm \frac{E_{max} - E_{min}}{E_{max} + E_{min}} \end{cases} \quad (5)$$

Where, E_{max} is the maximum value of irradiation; E_{min} is the minimum value of irradiation; E_{av} is the average value of irradiation; The closer the values of U_0 , U_1 and U_2 are to 1, the more uniform the light distribution is; *Bias* the larger the value, the more uneven the light distribution.

As shown in Fig. 3, it is the change of irradiation uniformity at the light outlet hole of the integrating sphere during the process

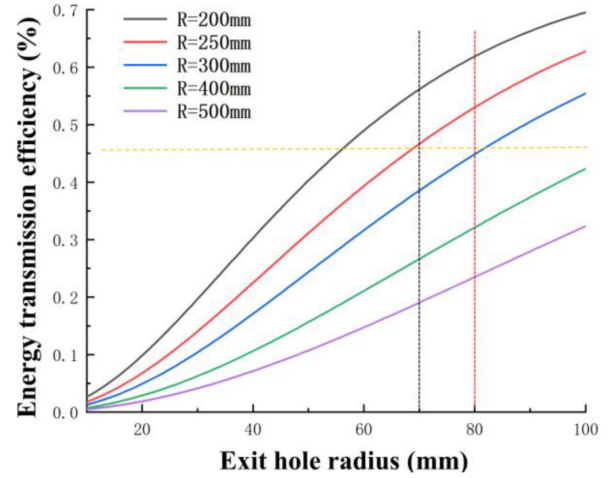


Fig. 4. Relationship between energy transmission efficiency and different light outlet hole radius and integrating sphere radius.

that the ratio of the opening size and radius of the integrating sphere changes from 10% to 50%.

As can be seen from the above figure, if the total opening of the integrating sphere is too large or too small, the irradiation uniformity will be reduced. The figure specifically shows the irradiation uniformity at the light outlet hole when the proportion is 30% and 40%, and between 30%–40%, U_0 , U_1 , U_2 is high, and the best radius of the light outlet hole of the integrating sphere is 55 mm–80 mm.

To sum up, considering the two factors of energy transmission efficiency and irradiation uniformity, the most suitable radius of the light outlet hole of the integrating sphere is 70–80 mm, and the ratio of the opening size and radius of the integrating sphere is 36%–40%. In this range, the relationship between energy transmission efficiency and the radius of the integrating sphere is shown in Fig. 4 in combination with (2), so as to analyze and determine the radius of the integrating sphere itself.

In the range of 70–80 mm of the optimal light outlet hole, if the energy transmission efficiency of the integrating sphere is to reach more than 45%, the radius of the integrating sphere is 200 and 250 mm. However, considering the actual volume and heat dissipation, the opening area of the integrating sphere is not more than 5% of the inner surface of the integrating sphere, and the radius of the light outlet hole is not more than 1/3 of the radius of the integrating sphere to ensure the uniform light effect [17], the radius of the integrating sphere is selected as 250 mm.

In order to finally determine the size of the light outlet hole of the integrating sphere, the intersection range is specifically analyzed. The irradiation uniformity of the integrating sphere is 97.84%–98.18%, and the energy transmission efficiency is between 46%–53%, both of which are relatively optimal. The influence of the size of the light outlet hole on the irradiation uniformity is shown in Fig. 5.

According to the above figure, the design result can be finally determined. The radius of the light outlet hole of the integrating sphere is 75 mm, which meets the intersection range of the optimal opening radius of the integrating sphere analyzed above.

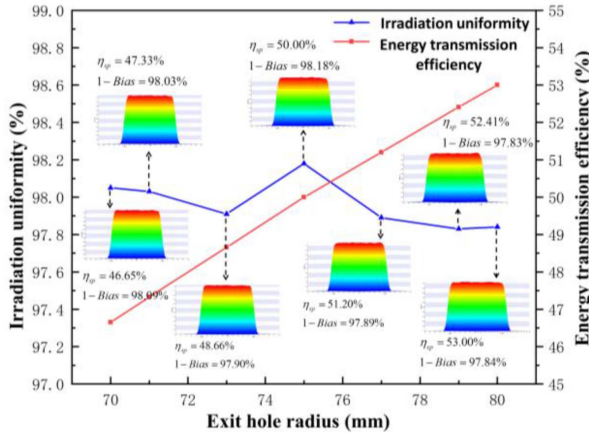


Fig. 5. Influence of the size of the light outlet hole of the integrating sphere in the range of 70–80 mm on the irradiation uniformity.

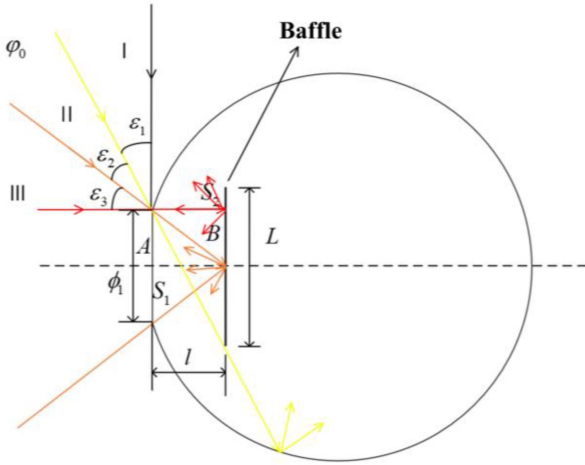


Fig. 6. Sectional view of integrating sphere light inlet.

At this time, the ratio of the opening size and radius of the integrating sphere is 38%, the ratio of the aperture area of the integrating sphere to the inner surface area of the integrating sphere is 2.41%, the irradiation uniformity at the light outlet hole of the integrating sphere is 98.18%, and the energy transmission efficiency is 50%.

C. Analysis and Design of the Influence of Baffle Size and Position on Irradiation Uniformity and Irradiance

The size and position of the baffle not only determines the uniform light effect of the integrating sphere, but also has a great influence on whether the incident light directly escapes from the light outlet hole. Generally speaking, in order not to affect the uniform light effect of the integrating sphere, the built-in items should not be too large [22].

As shown in Fig. 6, it is a cross-sectional view of the light entrance hole of the integrating sphere model. The incident light angle can be divided into three parts for analysis: In part I, when the incident angle of the incident light is less than ϵ_1 , that is, the angle between the incident angle and the horizontal axis is

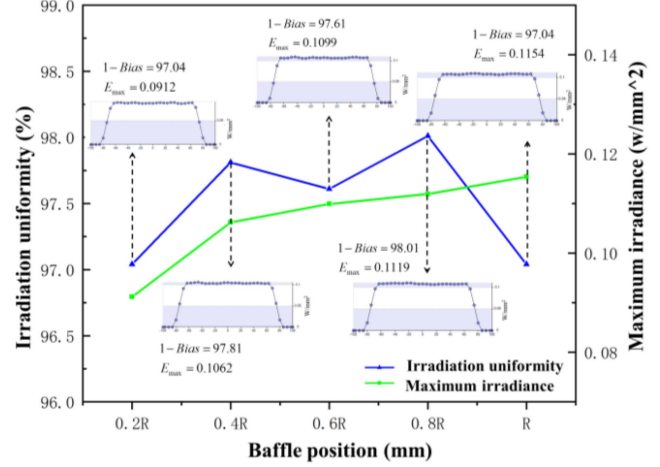


Fig. 7. Influence of different baffle positions on irradiation uniformity.

within $[\epsilon_2 + \epsilon_3, \frac{\pi}{2})$, all the light will enter the integrating sphere for the first diffuse reflection; In part II, when the incident angle of the incident light is less than ϵ_2 , that is, the angle between the incident angle and the horizontal axis is within $[\epsilon_3, \epsilon_2 + \epsilon_3]$, the light will first hit the baffle, and then be reflected to the inner wall of the integrating sphere for the second diffuse reflection; In part III, when the incident angle of the incident light is less than ϵ_3 , that is, the angle between the incident angle and the horizontal axis is within $[0, \epsilon_3]$, most of the light will escape from the integrating sphere through the light entrance hole of the integrating sphere.

According to the geometric conditions, the following relationship exists

$$\begin{cases} \epsilon_1 = \arctan\left(\frac{2l}{L + \phi_1}\right) \\ \epsilon_2 = \arctan\left(\frac{2l}{\phi_1}\right) - \arctan\left(\frac{2l}{L + \phi_1}\right) \\ \epsilon_3 = \arctan\left(\frac{\phi_1}{2l}\right) \end{cases} \quad (6)$$

Where, ϵ_1 is the included angle of the first part of light; ϵ_2 is the included angle of the second part of light; ϵ_3 is the included angle of the third part of the light; l is the distance from the baffle plate to the light entrance hole of the integrating sphere; L is the baffle diameter; ϕ_1 is the aperture of the integrating sphere.

As can be seen from Fig. 6 and (6), the smaller the baffle diameter L , the better, on the premise that the light source does not directly outlet the light outlet hole. Since the aperture of the integrating sphere's light outlet hole in this design needs to be connected with the subsequent system without light leakage, the baffle diameter L is a thin circular plate with the same size as the integrating sphere's light outlet hole $2r_j$, and the baffle coating is the same as the inner wall of the integrating sphere.

Baffle position l is divided into $l_1 = 0.2R$, $l_2 = 0.4R$, $l_3 = 0.6R$, $l_4 = 0.8R$ and $l_5 = R$ for simulation, the influence of baffle position on irradiation uniformity is shown in Fig. 7.

It can be seen from the above figure that when the baffle is at position $l_4 = 0.8R$, the irradiation distribution at the light outlet hole of the integrating sphere is the smoothest, that is, the irradiation uniformity is the highest, which is 98.01%; The

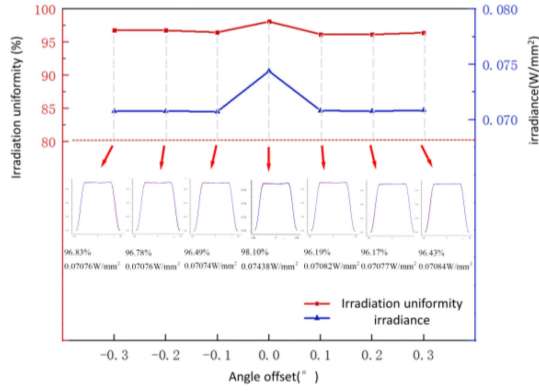


Fig. 8. Simulation results of angle error on irradiance and irradiation inhomogeneity at the light outlet hole.

smaller l is, the more light directly escapes from the light outlet hole of the integrating sphere, and the maximum irradiance after $l_4 = 0.8R$ is relatively high and stable. Therefore, the best position of the integrating sphere baffle is $l_4 = 0.8R$.

V. OPTICAL SYSTEM SIMULATION

A. Simulation Analysis of the Assembling and Adjusting Error of the Integrating Sphere

The installation and adjustment errors of integrating sphere mainly include angle error and displacement error [23], which are simulated and analyzed below.

1) *Influence of Angle Error on Irradiance and Irradiation Inhomogeneity at the Light Outlet Hole:* Take the upward deviation from the central optical axis of the optical system as a positive angle and the downward deviation from the central optical axis as a negative angle. Analyze the irradiance and irradiation non-uniformity of the light outlet when the integrating sphere deflects at different angles. The simulation results are shown in Fig. 8.

It can be seen from the figure that the angle error has a great impact on the irradiance and irradiation nonuniformity at the light outlet, and the angle error should be strictly controlled within the range of $(-0.1^\circ, 0.1^\circ)$. Beyond this range, the irradiance and irradiation nonuniformity will be greatly reduced.

2) *Effect of Displacement Error on Irradiance and Irradiation Inhomogeneity at the Light Outlet Hole:* Taking the displacement far from the light source as positive displacement and the displacement close to the light source as negative displacement, analyze the irradiance and irradiation non-uniformity at the light outlet when the integrating sphere is axially displaced. The simulation results are shown in Fig. 9. Taking the upward displacement away from the central optical axis of the optical system as the positive displacement and the downward displacement away from the central light as the negative displacement, the irradiance and irradiation non-uniformity at the light outlet of the integrating sphere during the radial displacement are analyzed. The simulation results are shown in Fig. 10.

It can be seen from the figure that when the integrating sphere deviates from the design position, both the axial displacement error and the radial displacement error have a greater impact on the irradiance and irradiation non-uniformity at the light

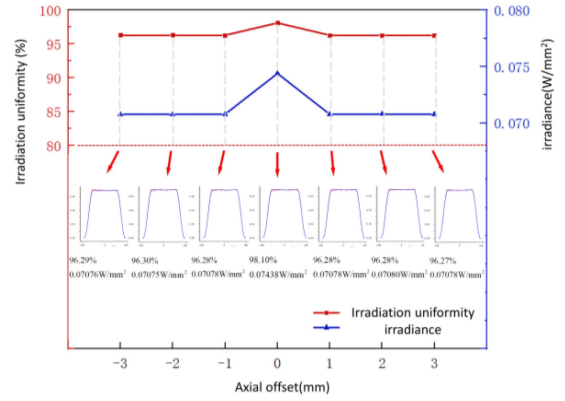


Fig. 9. Simulation results of axial displacement error on irradiance and irradiation inhomogeneity at the light outlet hole.

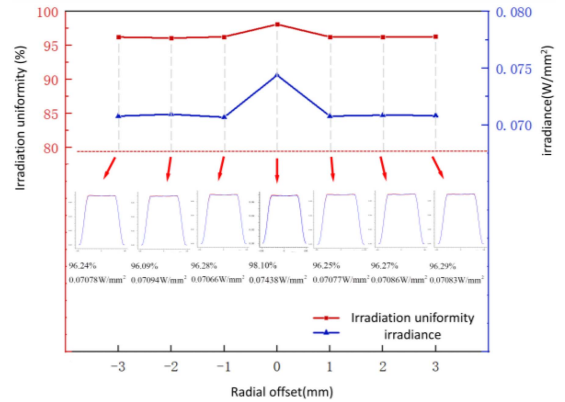


Fig. 10. Simulation results of radial displacement error on irradiance and irradiation inhomogeneity at the light outlet.

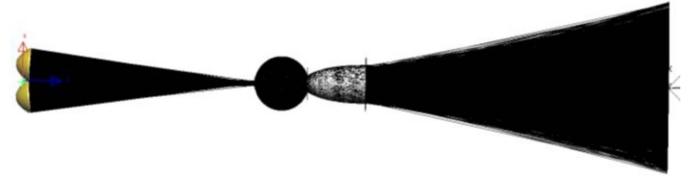


Fig. 11. Simulation diagram of overall optical system.

outlet. Therefore, the axial and radial displacement errors shall be strictly controlled within $(-1, 1)$ during assembly and adjustment. If they exceed this range, they will not meet the design requirements.

To sum up, the installation and adjustment accuracy of the integrating sphere is required to be high. In order to ensure the angle accuracy, axial displacement accuracy and radial displacement accuracy of the integrating sphere, the angle error range is $(-0.1^\circ, 0.1^\circ)$, the axial displacement error range is $(-1, 1)$ and the radial displacement error range is $(-1, 1)$.

B. System Overall Simulation Analysis

Use LightTools to build the simulation model of xenon lamp, ellipsoidal condenser, integrating sphere, baffle and composite parabolic reflector, as shown in Fig. 11.

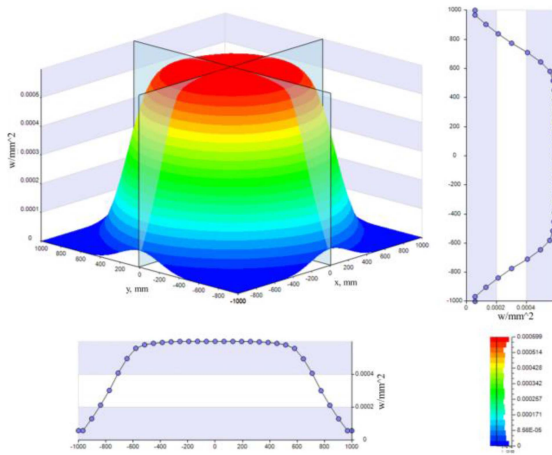


Fig. 12. Simulation result of the system.

The radius of the light entrance hole, the radius of the light outlet hole and the radius of the sphere are 20 mm, 75 mm and 250 mm respectively. The reflectance refers to the existing process, and the reflectance of the ellipsoidal condenser is directly set to 0.9; The simulated light source is two 3kw xenon lamps; The inner wall reflectance of the integrating sphere is 0.98; The reflectance of the composite parabolic reflector is 0.85. Monte Carlo ray tracing method is used to determine the luminous flux entering the receiver, the number of tracing rays is 20000000, and the display rays are 10000, ray tracing is carried out. Finally, the irradiation uniformity and irradiance of the irradiation surface not less than $\Phi 1000$ mm are calculated, and the simulation results are shown in Fig. 12.

Using the calculation (5) to calculate the irradiance non-uniformity, it can be obtained that in the effective irradiation surface of $\Phi 1032$ mm, the irradiance non-uniformity is 1.98%, and the maximum irradiance is $0.62S_0$, which realizes the solar irradiation simulation of high uniformity in the large irradiation surface.

VI. CONCLUSION

The irradiation uniformity of optical integrators under the influence of spherical aberration, side lobe effect and mutual restriction between irradiation surface and irradiance is studied. A method of using integrating sphere to replace optical integrator for uniform light and compound parabolic reflector for beam shaping is proposed. The effects of the opening size of integrating sphere, the radius size of integrating sphere and the size and position of baffle on energy transmission efficiency and irradiation uniformity are analyzed, a porous integrating sphere with high energy transmission efficiency and high irradiation uniformity is designed, and the spot simulation with high irradiation uniformity on a large irradiation surface is realized. The simulation results show that when the ratio of the aperture size to the radius of the integrating sphere is 36%–40%, $Bias$ and η_{sp} at the light outlet aperture are 97.84%–98.18% and 46%–53%, respectively; The best position of the baffle is $0.8R$ away from the light entrance hole. At this time, the irradiation non-uniformity at the light outlet hole is the lowest, with a value of 1.99%. In the optical system simulation of the solar simulator,

the irradiation non-uniformity is 1.98% and the maximum irradiance is $0.62S_0$ in the effective irradiation surface of $\Phi 1032$ mm. It has certain reference significance for the design and use of the integrating sphere used in the uniform light system of the solar simulator.

REFERENCES

- [1] L. Martínez-Manuel et al., "Optimization of the radiative flux uniformity of a modular solar simulator to improve solar technology qualification testing," *Sustain. Energy Technol. Assessments*, vol. 47, Oct. 2021, Art. no. 101372, doi: [10.1016/j.seta.2021.101372](https://doi.org/10.1016/j.seta.2021.101372).
- [2] D. Zhiqiang et al., "Optical design of large-area projection solar simulator," *Acta Optica Sinica*, vol. 37, no. 6, pp. 232–240, Jun. 2017, doi: [10.3788/AOS201737.0623003](https://doi.org/10.3788/AOS201737.0623003).
- [3] Z. Guoyu et al., "Analysis on irradiation uniformity of sun simulator," *Chin. J. Opt. Appl. Opt.*, vol. 2, no. 1, pp. 41–45, Feb. 2009, doi: [10.3969/j.issn.2095-1531.2009.01.007](https://doi.org/10.3969/j.issn.2095-1531.2009.01.007).
- [4] Z. Jigong, "Homogenization effect of the optical integrator," *Instrum. Manuf.*, vol. 6, pp. 12–15, 1983.
- [5] L. Zhiqiang et al., "Research on a new cluster-type optical integrator for solar simulator," *Laser Optoelectron. Prog.*, vol. 51, no. 12, 2014, Art. no. 122301, doi: [10.3788/LOP51.122301](https://doi.org/10.3788/LOP51.122301).
- [6] T. Katsuki and F. Satoji, "Lighting device, projection display device and optical integrator," China Patent CN101625104, Jan. 13, 2010.
- [7] Z. Jigong, "Problems related to improving the uniformity of optical integrator," *Opt. Precis. Eng.*, vol. 5, pp. 28–32, 1983.
- [8] A. Gallo et al., "High flux solar simulators for concentrated solar thermal research: A review," *Renewable Sustain. Energy Rev.*, vol. 77, pp. 1385–1402, Jan. 2017, doi: [10.1016/j.rser.2017.01.056](https://doi.org/10.1016/j.rser.2017.01.056).
- [9] W. Guoming, Z. Guoyu, and L. Shi, "Simulation analysis of optical integrator on irradiation uniformity," *Opt. Techn.*, vol. 39, no. 6, pp. 499–504, 2013, doi: [10.13741/j.cnki.11-1879/o4.2013.06.016](https://doi.org/10.13741/j.cnki.11-1879/o4.2013.06.016).
- [10] Z. Jie, "Studies on theoretical analysis and application of the optical systems for reflective projection displays," Ph.D. dissertation, Zhejiang Univ., Hangzhou, China, 2005.
- [11] L. Tao, F. Donghui, C. Xiaoyun, and L. Jie, "Effect of optical intergrator element lenses' number and shape on the lighting uniformity of solar simulator," *J. Optoelectron. Laser*, vol. 25, no. 10, pp. 1849–1853, Oct. 2014, doi: [10.16136/j.joel.2014.10.030](https://doi.org/10.16136/j.joel.2014.10.030).
- [12] Z. Ran et al., "Uniform illumination method for large-area divergent solar simulators," *Opt. Precis. Eng.*, vol. 27, no. 3, pp. 552–560, Mar. 2019, doi: [10.3788/OPE.20192703.0552](https://doi.org/10.3788/OPE.20192703.0552).
- [13] L. Yongzhi et al., "Spectral irradiance distribution of solar simulator," *Opt. Precis. Eng.*, vol. 3, no. 3, pp. 25–29, Jun. 1995.
- [14] R. Koshel, *Illumination Engineering: Design With Nonimaging Optics*. Hoboken, NJ, USA: Wiley, 2013.
- [15] F. Adam, T. Chhayly, and C. Le Ru Eric, "Quantitative theory of integrating sphere throughput: Comparison with experiments," *Appl. Opt.*, vol. 60, no. 18, pp. 5335–5344, 2021, doi: [10.1364/AO.428450](https://doi.org/10.1364/AO.428450).
- [16] M. Born and E. Wolf, *Principles of Optics: Electromagnetic Theory of Propagation, Interference and Diffraction of Light*, 7th (Expanded) ed. Cambridge, U.K.: Cambridge Univ. Press, 1978.
- [17] Labsphere Inc., "A guide to integrating sphere theory and applications," 2015. Accessed: Dec. 6, 2012. [Online]. Available: <http://www.labsphere.com/technical/technical-guides.aspx>
- [18] W. Jinjiang and Y. Zhiwen, "Application of random variables in integrating sphere design," *Acta Photonica Sinica*, vol. 30, no. 11, pp. 1406–1408, 2001.
- [19] M. Wenlong and Q. Yafeng, "Research on integrating sphere light hole brightness attenuation test system," *Infrared Technol.*, vol. 39, no. 4, pp. 317–322, 2017.
- [20] Q. Meng, Y. Li, and Y. Gu, "Dynamic mesh-based analysis of dynamic irradiance characteristics of solar simulator," *Optik*, vol. 126, pp. 4658–4664, Aug. 2015, doi: [10.1016/j.ijleo.2015.08.085](https://doi.org/10.1016/j.ijleo.2015.08.085).
- [21] Z. Ruimin, *Design and Optimization of Integral Spherical Uniform Light System*. Guiyang, China: Guizhou Univ., 2020, doi: [10.27047/d.cnki.ggudu.2020.001274](https://doi.org/10.27047/d.cnki.ggudu.2020.001274).
- [22] H. Omnia and S. N. H., "Distant-detector versus integrating sphere measurements for estimating tissue optical parameters: A comparative experimental study," *Optik*, vol. 247, Dec. 2021, Art. no. 167981, doi: [10.1016/j.ijleo.2021.167981](https://doi.org/10.1016/j.ijleo.2021.167981).
- [23] Z. Dongxu, *Design and Research on Optical System of Large Aperture Reflective Solar Simulator*. Changchun, China: Changchun Univ. of Sci. and Technol., 2022, doi: [10.26977/d.cnki.gccgc.2022.000255](https://doi.org/10.26977/d.cnki.gccgc.2022.000255).